

For Journal of Biochemistry, Regular paper, Biochemistry, Lipid Biochemistry

Degradation of glycosylinositol phosphoceramide during plant tissue homogenization

Yoshimichi Takai^{1#}, Rumana Yesmin Hasi^{1#}, Naoko Matsumoto¹, Chiho Fujita¹, Hanif Ali¹,
Junji Hayashi¹, Ryushi Kawakami¹, Mutsumi Aihara¹, Toshiki Ishikawa², Hiroyuki Imai³,
Mayuko Wakida⁴, Kazuya Ando⁴ and Tamotsu Tanaka^{1*}

¹Graduate School of Technology, Industrial and Social Sciences, Tokushima University,
Tokushima 770-8513, Japan

²Graduate School of Science and Engineering, Saitama University, Saitama 338-8570, Japan

³Graduate School of Natural Science, Konan University, Kobe 658-8501 Japan

⁴JTEKT Corporation, Kariya 448-8652 Japan

#Contribution: These authors contributed equally to this work.

Running Title: GIPC degradation in plants

***Correspondence**

Tamotsu Tanaka,

Graduate School of Technology, Industrial and Social Sciences, Tokushima University,
Tokushima 770-8513, Japan

Tel: +81 88 656 7249

E-mail: tanaka.tamotsu@tokushima-u.ac.jp

Abbreviations

DAG, diacylglycerol; DGDG, digalactosyldiglyceride; FFA, free fatty acid; GIPC, glycosylinositol phosphoceramide; GluCer, glucosylceramide; InoGly, inositol glycan; MGDG, monogalactosyldiglyceride; NPC, nonspecific phospholipase C; PA, phosphatidic acid; PC1P, phytoceramide 1-phosphate; PCer, phytoceramide; PC, phosphatidylcholine; PE, phosphatidylethanolamine, PI, phosphatidylinositol; PS, phosphatidylserine; PSH, phytoshingosine; PLC, phospholipase C; PLD, phospholipase D; SphM, sphingomyelin; SQDG, sulfoquinovosyldiglyceride; THAP, 2,4,6-trihydroxy-acetophenone; VLCFA, very long-chain fatty acid.

Summary

A convenient method for the determination of plant sphingolipids (glycosylinositol phosphoceramide, GIPC; glucosylceramide, GluCer; phytoceramide 1-phosphate, PC1P and phytoceramide, PCer) was developed. This method includes the extraction of lipids using 1-butanol, alkali hydrolysis with methylamine and separation by TLC. The amounts of sphingolipids in the sample were determined based on the relative intensities of standard sphingolipids visualized by primulin/ UV on TLC. Using this method, we found that almost all GIPC were degraded in response to tissue homogenization in cruciferous plants (cabbage, broccoli and *Arabidopsis thaliana*). The decrease in GIPC was compensated for by increases in PC1P and PCer, indicating that GIPC was degraded by hydrolysis at the D and C positions of GIPC, respectively. In carrot roots and leaves, most of GIPC degradation was compensated for by an increase in PCer. In rice roots, the decrease in GIPC was not fully explained by the increases in PC1P and PCer, indicating that enzymes other than phospholipase C and D activities operated. As the visualization of lipids on TLC is useful for detecting the appearance or disappearance of lipids, this method will be available for the characterization of metabolism of sphingolipids in plants.

Keywords

glycosylinositol phosphoceramide, phospholipase C, phospholipase D, phytoceramide, phytoceramide 1-phosphate.

Sphingolipids are major components of the plasma membrane of eukaryotic cells. The major sphingolipids in animals are sphingomyelin and glycosphingolipids, whereas the glycosylinositol phosphoceramide (GIPC) and glucosylceramide (GluCer) are major sphingolipids in plants [1]. Ceramide (Cer) forms the hydrophobic backbone of these sphingolipids. The predominant animal sphingolipid backbone is Cer, which is composed of sphingosine (*d*18:1) and very long-chain fatty acid (VLCFA)- or LCFA. On the other hand, phytoceramide (PCer), which is composed of phytosphingenine or phytosphingosine (*t*18:1 or *t*18:0) and long- or very long-chain α -hydroxy fatty acid (hVLCFA), serves as the predominant backbone of sphingolipids of plants [1-4]. In both organisms, Cer or PCer is intermediates of sphingolipid biosynthesis [5]. The Cer is also formed by the hydrolysis of sphingolipids as signaling molecules involved in the differentiation and apoptosis of animal cells [6]. It seems that hydrolysis-derived PCer play similar signaling roles in plant cells [5].

Previously, we identified an uncharacterized sphingolipid in cabbage homogenates as phytoceramide 1-phosphate (PC1P) [7], and found that the PC1P was formed from GIPC by hydrolysis at D position of the GIPC [7]. We named the enzymatic activity as GIPC-phospholipase D (GIPC-PLD) activity, and characterized it in several plants [8, 9]. Recently, we identified the GIPC-PLD protein in radishes as a protein encoded by a gene known as nonspecific phospholipase C3 (*NPC3*) [10]. The purified *NPC3* protein expressed in *Escherichia coli* was found to have the essentially the same enzymatic characteristics as GIPC-PLD activity in *Brassica* plants [10]. Another enzyme that has been characterized as GIPC-hydrolyzing enzyme is *NPC4*. Yang et al. identified *NPC4* as GIPC-PLC, and proposed that the role of *NPC4* is to supply of phosphorus during phosphate starvation in plants [11-13]. These results suggest that the hydrolysis of sphingolipids occurs in response to stress or environmental changes, such as wounding or nutritional deficiency in plants, by the activation of *NPC* enzymes. However, the exact mechanisms of GIPC degradation and the roles of the

hydrolytic products, such as PC1P, inositol glycan, PCer and phosphoinositol glycan, are largely unknown. Quantitative studies on sphingolipids under different plant conditions are helpful for understanding the roles of GIPC degradation. To this end, convenient methods for quantification of sphingolipids are useful to assessing the operation of those metabolism.

TLC is a convenient method for detecting all lipids and their relative abundances. It is also useful for detecting the appearance or disappearance of lipids in a sample. Recently, low-emission diode (LED) in the UV range have been used to enhance fluorescence intensity of detection reagents. In this study, we developed a convenient method to determine the plant sphingolipids, GIPC, PC1P, GluCer and PCer (Fig. 1) using a TLC-imaging technique. We showed that GIPC is degraded into PC1P and PCer in response to tissue homogenization in several plants.

Materials and Methods

Materials

GluCer from rice and N-(2'-(R)-hydroxylyngoceroyl)-phytosphingosine (PCer) from *Saccharomyces cerevisiae* were purchased from Avanti Polar Lipids (Alabaster, AL, USA). GIPC was isolated from the cabbage lipids using a previously described method [14]. Cabbage (*Brassica oleracea* L. var. *capitata*), broccoli (*Brassica oleracea* L. var. *italica*) were purchased from the local market. *Arabidopsis thaliana* was grown in soil and mature plants were utilized in experiments. Carrots (*Daucus carota* L.) were obtained from local farmers. Rice (*Oryza sativa*) was provided by JA Tokushima-shi (Tokushima, Japan). 2,4,6-Trihydroxy-acetophenone (THAP) was purchased from Sigma-Aldrich (St. Louis, MO, USA). Phos-tag containing Zn [⁶⁸Zn] was obtained from Wako Pure Chemical Industries (Osaka, Japan). The TLC plates used are Merck 5721, (Darmstadt, Germany). All organic solvents used in this study were of reagent grade and obtained from Nacalai Tesque Inc. (Tokyo, Japan).

Homogenization of plant tissues

Fresh plant tissues (0.3-3 g wet weight), such as roots, leaves, and stems, were isolated and cut into small pieces. After adding an equal amount of cold water, the tissues were homogenized using an ultra-disperser (LK-21; Yamato Scientific, Tokyo, Japan) for 3 min at room temperature. As the degradation of sphingolipids is a rapid process, heat treatment was performed before homogenization to inactivate the plant enzymes. The fresh plant tissues (0.3-3g wet weight) were wrapped with aluminum foil, placed in a steam cooker and heated for 10 min. After cooling and wiping off moisture, the tissues were homogenized as described above. The sphingolipid composition of the heat-treated plant samples was regarded as that before homogenization.

Lipid extraction and TLC

Total lipids were extracted from the homogenates using a two-phase solvent system, consisting of 1-butanol and water (1:1, v/v) [15]. The butanol phase was collected after centrifugation at $1100 \times g$ for 5 min. The solvent was removed with an evaporator at 50 °C. The extracted lipids were treated with 40% methylamine/ethanol (5:7, v/v) for 2 h at 50 °C to hydrolyze the glycerophospholipids. After evaporation, the resulting extracts were dissolved in a small amount of the lower layer of isopropanol/hexane/water (55:20:25, v/v/v; solvent A) and subjected to TLC. The solvent system used for the separation of GIPC and PC1P was chloroform/methanol/7% aqueous ammonia (45:35:10, v/v/v). For separation of GluCer, it was chloroform/methanol/acetic acid (85:15:1, v/v/v). For separation of PCer, it was chloroform/methanol/acetic acid (90:6:1, v/v/v). The TLC plate was dried by blowing air and sprayed with primulin (0.01% in 80% acetone) to visualize the lipids on the plate under a UV light. To enhance the detection sensitivity, UV-LED light was used. When isolating GIPC for MALDI-TOF MS, the silica gel corresponding to GIPC was scraped off the TLC plate, mixed with solvent A, and sonicated for few seconds. GIPC was recovered from the supernatant after centrifugation at $1,300 \times g$ for 5 min. Purified PC1P was also obtained by TLC. The PC1P was recovered from the silica gel according to the Bligh and Dyer method [16] with acidification of the methanol/water phase [14]. The isolated GIPC and PC1P were quantified by colorimetric method based on phosphomolybdenum-malachite green formation and subjected to MALDI-TOF MS [14]. When isolating PCer and GluCer, we used the Bligh and Dyer method [16] for their extraction from the scraped silica gel. The isolated sphingolipids were subjected to MALDI-TOF MS for structural and compositional analysis as described below.

Quantification of sphingolipids by TLC imaging:

The quantification of the sphingolipids was based on the pixel intensity value (PIV) of the digital images of GIPC, PC1P, GluCer and PCer spots on the TLC plate. The PIV of the spots was determined using ImageJ software (NIH, Bethesda, MD, USA). The amounts of these lipids were quantified based on their PIV values relative to those of the standard lipid bands [17].

MALDI-TOF MS

The structure of GIPC from cabbage was analyzed by MALDI-TOF MS (Bruker Daltonics, Bremen, Germany) in the negative-ion detection mode [14], whereas, GluCer and PCer were determined in the positive-ion detection mode. A THAP solution (10 mg/mL in 75% acetonitrile containing 0.1% trifluoroacetic acid) was used as the matrix. The wave-length of the nitrogen-emitting laser, the pressure in the ion chamber, and the accelerating voltage were 337 nm, 3.7×10^{-7} Torr, and 20 kV, respectively. The molecular species of PC1P were determined by MALDI-TOF MS using a Phos-tag, as previously described [7]. An aliquot of PC1P was dissolved in 100 μ L of methanol containing 0.3% ammonia. The resulting solution (10 μ L) was mixed with 5 μ L of 0.1 mM ^{68}Zn phos-tag solution and a small portion (0.5 μ L) of this mixture was spotted on the MALDI sample plate. Immediately, 0.5 μ L of the 2,4,6-trihydroxyacetophenone (THAP) solution (10 mg/mL in acetonitrile) was layered onto the mixture as a matrix solution. After drying the sample plate for a few minutes, the matrix/analyte was subjected to MALDI-TOF MS in positive-ion detection mode.

Statistical analysis

All results are expressed as mean \pm SD. The significant differences between two means were determined using Student's *t*-test. **P* < 0.05, ***P* < 0.01, and ****P* < 0.001 were defined as statistically significant.

Results

TLC of plant lipids

The method of Bligh and Dyer [16] is commonly used for the extraction of sphingolipids from biological materials. However, it is not applicable for extraction of GIPC, because of the low solubility of GIPC in the chloroform layer [14]. In fact, the amount of GIPC obtained from cabbage leaves using Bligh and Dyer extraction is around 10 nmol/g (wet weight), which is less than 10% as compared to our reported method using solvent A [14]. In this study, we extracted the plant lipids using 1-butanol as reported by Buré al. [15]. Although 1-butanol is hard to evaporate as compared to isopropanol or chloroform, the 1-butanol extraction is advantageous in simultaneous extraction of GIPC, GluCer, PC1P and PCer. We found that amount of GIPC obtained from cabbage leaves is 100-200 nmol/g (wet weight), which is higher than that obtained using solvent A (around 100 nmol/g wet weight) [14]. Additional improvement is application of UV-LED light for detection of primulin positive band on TLC. As shown in supplementary Fig. 1, fluorescence of each band detected under UV-LED is brighter than that under normal UV light. The clear boundary of each lipid band is helpful for TLC-image based quantification.

The lipids extracted from the heat-treated cabbage leaves were separated using TLC as shown in Fig. 2. GIPC and PC1P were separated from the other lipids by TLC using solvent system chloroform/methanol/7% aqueous ammonia (45:35:10, v/v/v). GluCer was separated using chloroform/methanol/acetic acid (85:15:1, v/v/v). The solvent system chloroform/methanol/acetic acid (90:6:1, v/v/v) was used for the separation of PCer. We performed alkaline hydrolysis of the extracted lipids with methylamine for decomposition of coexisting glycerolipids. This procedure is recommended for avoidance of contamination of glycerolipid to the sphingolipid bands as shown in the Fig. 2.

Isolated GIPC, PC1P, GluCer and PCer were subjected to MALDI-TOF/MS for structural confirmation. As shown in Fig. 2A, GIPC species containing two sugars (GIPC Series A or S2 GIPC) and GIPC species containing three sugars (GIPC Series B or S3 GIPC) were present in cabbage leaves. They were assigned as GIPCs having phytosphingenine (*t*18:1) and α -hydroxy fatty acids with chain-length of C16~C24 as *N*-acyl residues (Fig. 3A, B, Table 1). PC1P is a sphingolipid formed in response to homogenization. The molecular species composition of PC1P in cabbage was similar to that of S2 GIPC (Fig. 3C, Table 1). These results were consistent with those of our previous study [14]. The assignments of GluCer with LCFA and GluCer with VLCFA observed by TLC (Fig. 2B) were based on the mass spectrometric analyses. The former could be assigned as GluCer having phytosphingenine (*t*18:1) and α -hydroxy fatty acids with chain-length of C16:1h, whereas, the latter could be assigned as GluCer containing C24:1h (Fig. 3D, E, Table 1). These assignments were based on the results reported by [2]. We detected only 2 species of PCer. These were assignable to phytosphingenine (*t*18:1) with α -hydroxy fatty acids with chain lengths of C22:0h and C24:1h (Fig. 3F, Table 1).

Determination of sphingolipids by TLC imaging

Previously, we developed a method for quantifying plant phospholipids, such as phosphatidic acid and phosphatidylcholine, using TLC imaging technique [17]. This is based on the fact that the intensity of the primulin/UV-induced fluorescence is proportional to the amount of lipids present in the band on TLC. To apply this methodology for quantification of GIPC, PC1P, GluCer and PCer, the relationship between the intensity of the primulin/UV-induced fluorescence and the amount of each sphingolipid was examined. Different amounts of standard sphingolipids up to 20 nmol were applied to TLC plates with width of approximately 1 cm. After developing the TLC plate, the lipid bands were visualized by

primulin/UV and digitized using ImageJ software. The results showed a proportional relationship between the amount of lipids and the fluorescence intensity detected by primulin/UV for all sphingolipids tested (Fig. 4). Based on these results, the amounts of the sphingolipids in the samples was determined using the relative value of the intensity of a known amount of standard band developed in the same TLC plate. We confirmed that the amount of GIPC and PC1P quantified by this TLC-imaging technique were similar to those obtained by the conventional colorimetric method based on phosphomolybdenum-malachite green formation [18].

Compositional change in sphingolipids during plant tissues homogenization

Compositional changes in sphingolipids in the plant tissue before (heat-treated sample) and after (raw sample) homogenization were examined using the TLC-imaging technique (Fig. 5). When cabbage leaves and stems were homogenized, increases of PC1P and PCer were observed along with an almost complete disappearance of GIPC (Fig. 5A, C). As the sum of the increments in PC1P and PCer was almost equal to the decrease in GIPC (Fig. 5D), PC1P and PCer produced in response to homogenization were considered to be derived from GIPC. It should be noted that Series A (S2) GIPC but not Series B (S3) GIPC was preferentially degraded as shown in Fig. 5A. This is consistent with our previous observation that cabbage GIPC-PLD shows activity toward Series A (S2) GIPC but not toward Series B (S3) GIPC [14]. The amounts of GluCer was not significantly altered by homogenization in any of the cabbage tissues (Fig. 5B, D).

The degradation of GIPC and the formations of PC1P and PCer were also observed in other cruciferous plants, such as broccoli (root and stem) and *Arabidopsis* (root and leaf) (Fig. 6A, B, Supplement Fig. 1, 2). Although the extent of GIPC degradation was lower than that in cruciferous plants, the formation of PC1P and PCer was observed in the roots and leaves of

carrots. In carrots, the conversion of GIPC to PCer appeared to proceed preferentially than that from GIPC to PC1P (Fig. 6C, Supplement Fig. 3). In rice root, the decrease in GIPC exceeded the sum of the increments in PC1P and PCer. This suggests that PC1P and PCer undergo further degradation in the tissues (Fig. 6D, Supplement Fig. 4).

We also examined the time-dependent changes in sphingolipids during the homogenization of cabbage leaves (Fig. 7). In this experiment, frozen cabbage leaves were used because degradation of GIPC is a rapid process that is difficult to control at room temperature. The results showed that a decrease in the GIPC involved a concomitant increase in the amounts of PC1P and PCer, whereas GluCer remained unchanged throughout the incubation period. Interestingly, PCer formation was slower than PC1P formation (Fig. 7C, G).

Discussion

Previously, we identified an uncharacterized sphingolipid in the homogenates of cabbage leaves as PC1P [7]. This observation led us to the finding that GIPC-hydrolyzing PLD is present in cabbage tissue [7-9] and that NPC3 is one of the enzymes responsible for GIPC-hydrolyzing PLD activity [10]. This is a good example showing that examination of compositional changes in sphingolipids during the homogenization of plant tissues provides insight into the GIPC degradation pathways. In this study, we developed a method for the quantitative analysis of sphingolipids using TLC-imaging technique, and investigated the compositional changes in sphingolipids in plant tissue during homogenization.

Here, we demonstrated that degradation of GIPC and formation of PC1P occur not only in the cruciferous plants but also in other plants such as rice (*Oriza sativa*) roots and carrot (*Daucus carota*) leaves and roots. This indicates that these plants contain GIPC-degrading enzymes (Fig. 8). In fact, NPC gene family is present in the genome of rice [19]. Although we do not know whether PC1P formation can be explained only by NPC3 activity, NPC3 has been shown to be expressed at high level in the roots of Arabidopsis [20], and is involved in root development [21]. These facts are consistent with those of our previous study [8] and the current observations that PC1P formation was higher in roots than in other tissues in all plants tested.

In the present study, we observed that GIPC degradation was involved in the PCer production in all plants. The decrease in GIPC was similar level to the sum of the increase in PC1P and PCer in cruciferous plants, indicating that PCer and PC1P are formed from GIPC (Fig. 8). In this regard, NPC4 has been characterized as GIPC-hydrolyzing PLC in *Arabidopsis* [11-13]. The NPC4 gene is found in several plants including radish and rice [10, 22]. Therefore, NPC4 is a potential enzyme that explains the PCer formation from GIPC. Similar to NPC3, mRNA of NPC4 has been shown to present abundantly in roots [20, 21], and is involved in

root growth [11], which is consistent with the observation that PCer formation is higher in the roots than that in the leaves of cruciferous plants. We also observed the PCer formation in rice and carrots. Although the expression level is considerably lower in other NPC family members, the expression of NPC4 is observed only in roots of rice [22].

Another mechanism that explains PCer formation is the dephosphorylation of PC1P by phosphatases (Fig. 8). Many organisms including plants possess nonspecific phosphatase [23]. PC1P may be converted to PCer during homogenization by the phosphatase activity. In this regard, it should be mentioned that PCer formation was slower than PC1P formation as shown in Fig. 7.

Ceramide kinase activity has been shown in plants [24]. Although the ceramide kinase route is not likely to be a main route for PC1P formation during homogenization, contribution of ceramide kinase pathway to the PC1P formation can not be ruled out. Contribution of PCer synthesized by de novo route is also possible. Because, it is known that de novo synthesis of ceramide proceeds in the apoptotic cell death in animal cells [25]. Further studies are needed for understanding the exact mechanisms of PC1P and PCer formation during homogenization of plant tissues.

The compositional change in sphingolipids of rice shoot is interesting in that PCer formation does not involve in the significant decrease in the amount of GIPC (Fig. 5D), This result indicated existence of PCer producing pathways, which are distinct from GIPC hydrolysis, in rice shoot. Since structure of GIPC of monocots (mainly Series B, S3 GIPC) is different from that of eudicots (mainly Series A, S2 GIPC) [26], rice shoot may have metabolic pathways that are distinct from eudicots.

PLD activity acting on glycerophospholipids in plants was discovered in 1948 [27]. Since then, many species of PLD have been identified, and their structures, regulatory mechanisms, and physiological roles have been clarified [28]. Currently, it is established that plant PLDs

acting on glycerophospholipids play important roles in stress and hormone responses by producing phosphatidic acid (PA) as an intracellular signaling molecule [29]. In the present study, we showed that a significant portion of GIPC, the most abundant sphingolipid in plants, is degraded in response to the homogenization, leading to PC1P and PCer formation. However, the physiological significance of the degradation of GIPC and production of the lysates remains unknown. We hope that this convenient method for the determination of plant sphingolipids by TLC imaging will contribute to research for clarification of physiological significance of sphingolipid metabolism in plants.

References

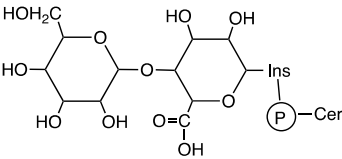
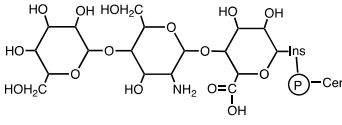
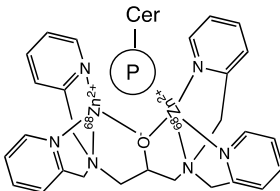
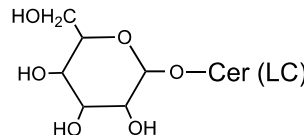
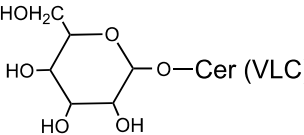
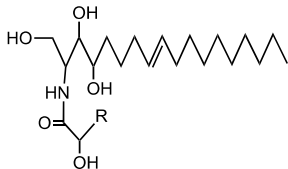
1. Markham, J.E., Li, J., Cahoon, E.B., and Jaworski, J.G. (2006) Separation and identification of major plant sphingolipid classes from leaves. *J. Biol. Chem.* **281**, 22684–22694
2. Cacas, J.L., Furt, F., Le Guédard, M., Schmitter, J.M., Buré, C., Gerbeau-Pissot, P., Moreau, P., Bessoule, J.J., Simon-Plas, F., and Mongrand, S. (2012) Lipids of plant membrane rafts. *Prog. Lipid Res.* **51**, 272-299
3. Sperling, P., and Heinz, E. (2003) Plant sphingolipids: structural diversity, biosynthesis, first genes and functions. *Biochim. Biophys. Acta.* **1632**, 1-15
4. Gronnier, J., Germain, V., Gouguet, P., Cacas J.L., and Mongrand S. (2016) GIPC: Glycosyl Inositol Phospho Ceramides, the major sphingolipids on earth. *Plant Signal Behav.* **11**, e1152438
5. Liu, N.J., Hou, L.P., Bao, J.J., Wang, L.J., Chen, X.Y. (2021) Sphingolipid metabolism, transport, and functions in plants: Recent progress and future perspectives. *Plant Commun.* **2**, 100214
6. Hannun, Y.A., and Obeid, L.M. (2018) Sphingolipids and their metabolism in physiology and disease. *Nat. Rev. Mol. Cell Biol.* **19**, 175-191
7. Tanaka, T., Kida, T., Imai, H., Morishige, J., Yamashita, R., Matsuoka, H., Uozumi, S., Satouchi, K., Nagano, M., and Tokumura, A. (2013) Identification of a sphingolipid-specific phospholipase D activity associated with the generation of phytoceramide-1-phosphate in cabbage leaves. *FEBS J.* **280**, 3797-3809
8. Kida, T., Itoh, A., Kimura, A., Matsuoka, H., Imai, H., Kogure, K., Tokumura, A., and Tanaka, T. (2017) Distribution of glycosylinositol phosphoceramide-specific phospholipase D activity in plants. *J. Biochem.* **162**, 449-458

9. Hasi, R.Y., Miyagi, M., Morito, K., Ishikawa, T., Kawai-Yamada, M., Imai, H., Fukuta, T., Kogure, K., Kanemaru, K., Hayashi, J., Kawakami, R., and Tanaka, T. (2019) Glycosylinositol phosphoceramide-specific phospholipase D activity catalyzes transphosphatidylation. *J. Biochem.* **166**, 441–448
10. Hasi, R.Y., Ishikawa, T., Sunagawa, K., Takai, Y., Ali, H., Hayashi, J., Kawakami, R., Yuasa, K., Aihara, M., and Tanaka, T. (2022) Nonspecific phospholipase C3 of radish has phospholipase D activity towards glycosylinositol phosphoceramide. *FEBS Lett.* **596**, 3024-3036
11. Yang, B., Li, M., Phillips, A., Li, L., Ali, U., Li, Q., Lu, S., Hong, Y., Wang, X., and Guo, L. (2021) Non-specific phospholipase C4 hydrolyzes phosphosphingolipids and sustains plant root growth during phosphate deficiency. *Plant Cell.* **33**, 766-780
12. Yang, B., Zhang, K., Jin, X., Yan, J., Lu, S., Shen, Q., Guo, L., Hong, Y., Wang, X., and Guo, L. (2021) Acylation of nonspecific phospholipase C4 determines its function in plant response to phosphate deficiency. *Plant J.* **106**, 1647-1659
13. Fan, R., Zhao, F., Gong, Z., Chen, Y., Yang, B., Zhou, C., Zhang, J., Du, Z., Wang, X., Yin, P., Guo, L., and Liu, Z. (2023) Insights into the mechanism of phospholipid hydrolysis by plant nonspecific phospholipase C. *Nat. Commun.* **14**, 194
14. Hasi, R.Y., Majima, D., Morito, K., Ali, H., Kogure, K., Nanjundan, M., Hayashi, J., Kawakami, R., Kanemaru, K., and Tanaka, T. (2020) Isolation of glycosylinositol phosphoceramide and phytoceramide 1- phosphate in plants and their chemical stabilities. *J. Chromatogr. B.* **1152**, 122213
15. Buré, C., Cacas J-L, Mongrand, S. and Schmitter, J-M. (2014) Characterization of glycosyl inositol phosphoryl ceramides from plants and fungi by mass spectrometry. *Anal. Bioanal. Chem.* **406**, 995–1010

16. Bligh, E.G. and Dyer, W.J. (1959) A rapid method of total lipid extraction and purification. *Can. J. Biochem. Physiol.* **37**, 911-917
17. Tanaka, T., Kassai, A., Ohmoto, M., Morito, K., Kashiwada, Y., Takaishi, Y., Urikura, M., Morishige, J., Satouchi, K., and Tokumura, A. (2012) Quantification of Phosphatidic Acid in Foodstuffs Using a Thin-Layer-Chromatography-Imaging Technique. *Agric. Food Chem. J.* **16**, 4156–4161
18. Chalvardjian, A., and Rudnicki, E. (1970) Determination of lipid phosphorus in the nanomolar range. *Anal. Biochem.* **36**, 225-230
19. Nakamura, Y., and Ngo, A.H. (2020) Non-specific phospholipase C (NPC): an emerging class of phospholipase C in plant growth and development. *J. Plant Res.* **133**, 489–497
20. Peters, C., Li, M., Narasimhan, R., Roth, M., Welti, R., and Wang, X. (2010) Nonspecific phospholipase C NPC4 promotes responses to abscisic acid and tolerance to hyperosmotic stress in *Arabidopsis*. *Plant Cell* **22**, 2642–2659
21. Wimalasekera, R., Pejchar, P., Holka, A., Martinec, J., and Scherer, G.F.E. (2010) Plant phosphatidylcholine-hydrolyzing phospholipases C NPC3 and NPC4 with roles in root development and brassinolide signaling in *Arabidopsis thaliana*. *Molecular Plant* **3**, 610–625
22. Cao, H., Zhuo, L., Su, Y., Sun, L., and Wang, X. (2016) Non-specific phospholipase C1 affects silicon distribution and mechanical strength in stem nodes of rice. *Plant J.* **86**, 308-321
23. Moorhead, G.B., De Wever, V., Templeton, G., and Kerk, D. (2009) Evolution of protein phosphatases in plants and animals. *Biochem. J.* **417**, 401-409
24. Bi, F-C., Zhang, Q-F., Liu Z., Fang, C., Li, J., Su, J-B., Greenberg, J.T., Wang, H-B., and Yao, N. (2011) A conserved cysteine motif is critical for rice ceramide kinase activity and function. *PLoS One* **6**, e18079

25. Morad, S.A.F., and Cabot, M.C. (2013) Ceramide-orchestrated signaling in cancer cells. *Nature Rev.* **13**, 51-65
26. Lenarčič, T., Albert, I., Höhm, H., Hodnik, V., Pirc, K., Zavec, A.B., Podobnik, M., Pahovnik, D., Žagar, E., Pruitt, R., Greimel, P., Yamaji-Hasegawa, A., Kobayashi, T., Zienkiewicz, A., Gömann, J., Mortimer, J.C., Fang, L., Mamode-Cassim, A., Deleu, M., Lins, L., Oecking, C., Feussner, I., Mongrand, S., Anderluh, G., and Nürnberger, T. (2017) Eudicot plant-specific sphingolipids determine host selectivity of microbial NLP cytolysins. *Science* **358**, 1431-1434
27. Hanahan, D.J., and Chaikoff, I.L. (1984) On the nature of the phosphorus-containing lipides of cabbage leaves and their relation to a phospholipide-splitting enzyme contained in these leaves. *J. Biol. Chem.* **172**, 191-198
28. Selvy, P.E., Laveri, R.R., Lindsley, C.W., and Brown, H.A. (2011) Phospholipase D: enzymology, functionality, and chemical modulation. *Chem. Rev.* **111**, 6064-6119
29. Li, M., Hong, Y., and Wang, X. (2009) Phospholipase D- and phosphatidic acid-mediated signaling in plants. *Biochim Biophys Acta* **1791**, 927-935

Table 1. Ions detected in MALDI-TOF mass spectra and their possible assignments.

Sphingolipids	Structure of sphingolipids	Exact mas	Observed mas (<i>m/z</i>)	Possible assignments of ceramide moieties
GIPC S2 (Series A)		1148.6	1148.7	<i>t</i> 18:1/ <i>h</i> 16:0
		1232.7	1232.9	<i>t</i> 18:1/ <i>h</i> 22:0
		1246.7	1246.9	<i>t</i> 18:1/ <i>h</i> 23:0
		1258.7	1258.9	<i>t</i> 18:1/ <i>h</i> 24:1
		1260.7	1260.9	<i>t</i> 18:1/ <i>h</i> 24:0
		1281.7	1281.9	<i>t</i> 18:1/ <i>h</i> 24:1 + Na ⁺
GIPC S3 (Series B)		1421.8	1421.1	<i>t</i> 18:1/ <i>h</i> 24:1
		1422.8	1423.1	<i>t</i> 18:1/ <i>h</i> 24:0
		1445.8	1445.1	<i>t</i> 18:1/ <i>h</i> 24:0 + Na ⁺
		1450.8	1451.1	<i>t</i> 18:1/ <i>h</i> 26:0
PC1P with phos-tag		1236.6	1236.7	<i>t</i> 18:1/ <i>h</i> 16:0
		1320.6	1320.7	<i>t</i> 18:1/ <i>h</i> 22:0
		1334.6	1334.7	<i>t</i> 18:1/ <i>h</i> 23:0
		1346.6	1346.7	<i>t</i> 18:1/ <i>h</i> 24:1
		1348.7	1348.7	<i>t</i> 18:1/ <i>h</i> 24:0
		1362.7	1362.7	<i>t</i> 18:1/ <i>h</i> 25:0
GluCer LC		754.5	754.5	<i>t</i> 18:1/ <i>h</i> 16:1 + Na ⁺
		770.5	770.5	<i>t</i> 18:1/ <i>h</i> 16:1 + K ⁺
		864.7	864.6	<i>t</i> 18:1/ <i>h</i> 24:1 + Na ⁺
GluCer VLC		864.7	864.6	<i>t</i> 18:1/ <i>h</i> 24:1 + Na ⁺
		880.7	880.6	<i>t</i> 18:1/ <i>h</i> 24:1 + K ⁺
PCer		676.6	676.6	<i>t</i> 18:1/ <i>h</i> 22:0 + Na ⁺
		702.6	702.6	<i>t</i> 18:1/ <i>h</i> 24:1 + Na ⁺

Legend to Figures

Fig. 1 Typical structure of PCer, GluCer, GIPC and PC1P in cruciferous plants.

Phytoceramide composed of phytosphingenine (*t*18:1) and α -hydroxy nervonic acid (24:0h) is the typical backbone of GluCer, GIPC and PC1P in cabbage. GIPC having two sugars (mannose-glucuronic acid) is the predominant type in cruciferous plants.

Fig. 2. TLC of plant sphingolipids

The frozen cabbage leaves were homogenized. Lipids were extracted and treated with (alkali) or without (non) methylamine. The resulting lipids were separated by TLC by indicated solvent systems. Assignments of respective bands were performed co-migration on TLC with standard lipids, or MALDI TOF-MS.

Fig. 3. MALDI TOF-MS of sphingolipids in cabbage lipids.

S2 (upper band) and S3 (lower band), GIPC, PC1P, GluCer (lower band), GluCer (upper band) and PCer were isolated from the cabbage lipid by TLC as shown in Fig. 2. The isolated lipids were subjected to MALDI-TOF MS as described in the Materials and Methods. The possible assignments of the major ions detected in the mass spectrum are shown in Table 1.

Fig. 4. Relationship between the amount of sphingolipid and pixel intensity of the lipid band visualized on TLC.

Different amounts of standard sphingolipids (GIPC, PC1P, GluCer, and PCer) were applied to a TLC plate and developed as described in the Materials and Methods. The TLC image was captured by digital camera after visualizing the lipid bands using primulin/UV. The intensity of the band was quantified using ImageJ software and is shown as pixel intensity.

Fig. 5. Change in the sphingolipid contents of cabbage tissues during homogenization.

Homogenates of the cabbage tissues were prepared after treatment with (steam) or without (raw) steam. Lipids were extracted, treated with methylamine, and separated by TLC (A-C). Sphingolipids were quantified by TLC imaging and are expressed as nmol/g (wet weight) in D.

Fig. 6. Change in the sphingolipid contents of tissues of broccoli (A), *Arabidopsis* (B), carrot (C) and rice (D) during homogenization.

Homogenates of tissues of the plants were prepared after treatment with (steam) or without (raw) steam. Lipids were extracted, treated with methylamine, and separated by TLC. Sphingolipids were quantified by TLC imaging and are shown as nmol/g (wet weight).

Fig. 7. Time-dependent change in the sphingolipids during homogenization of cabbage leaves.

The young leaves of cabbage were frozen at -80 °C for overnight. After quick clashing and homogenization, the homogenates were incubated at 30 °C for indicated times. The lipids were extracted from the homogenates after steam treatment. The sphingolipids were separated by TLC (A, D, F), quantified by TLC imaging and are shown as nmol/g (wet weight) (B, C, E, G).

Fig. 8. Possible degradation pathway of GIPC in response to homogenization in plants.

Supplemental Fig. 1.

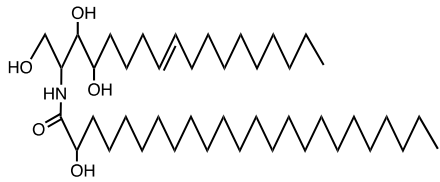
Visualization of GIPC and PC1P band on TLC with primulin/normal UV light and primulin/UV LED light.

Supplemental Fig. 2-4.

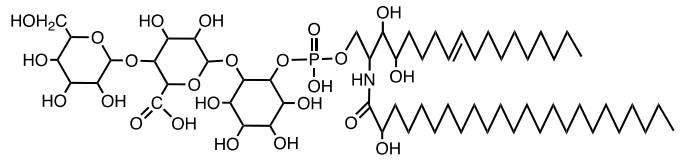
Typical TLC of sphingolipids of broccoli (Fig. 2), Arabidopsis (Fig. 3), carrot (Fig. 4) and rice (Fig. 5). The dark spots appeared on TLC are certain kinds of plant dyes which are seen as green or yellow band under visual light.

Fig. 1

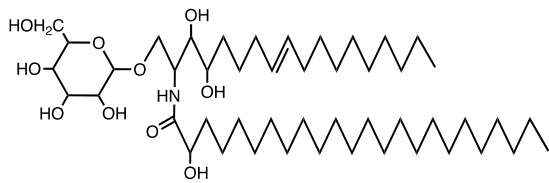
Phytoceramide (PCer)



Glycosylinositol phosphoceramide (GIPC)



Glucosylceramide (GluCer)



Phytoceramide 1-phosphate (PC1P)

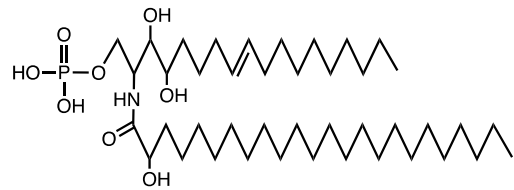


Fig. 2

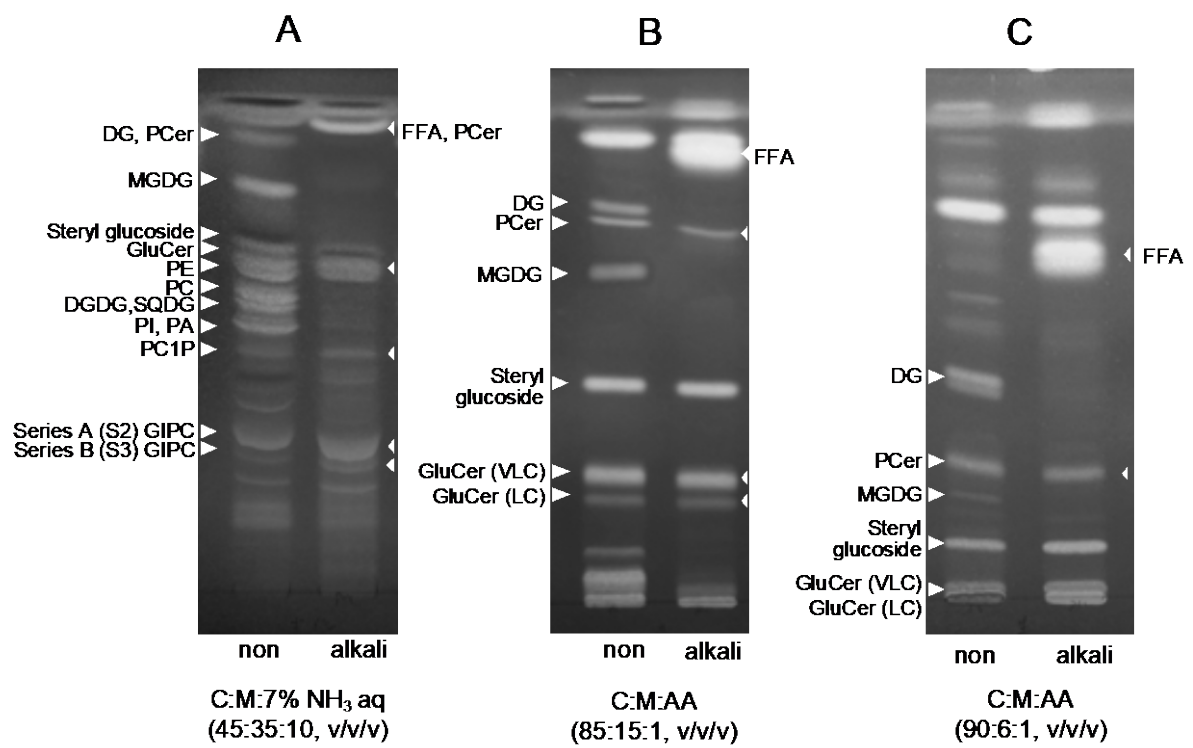


Fig. 3

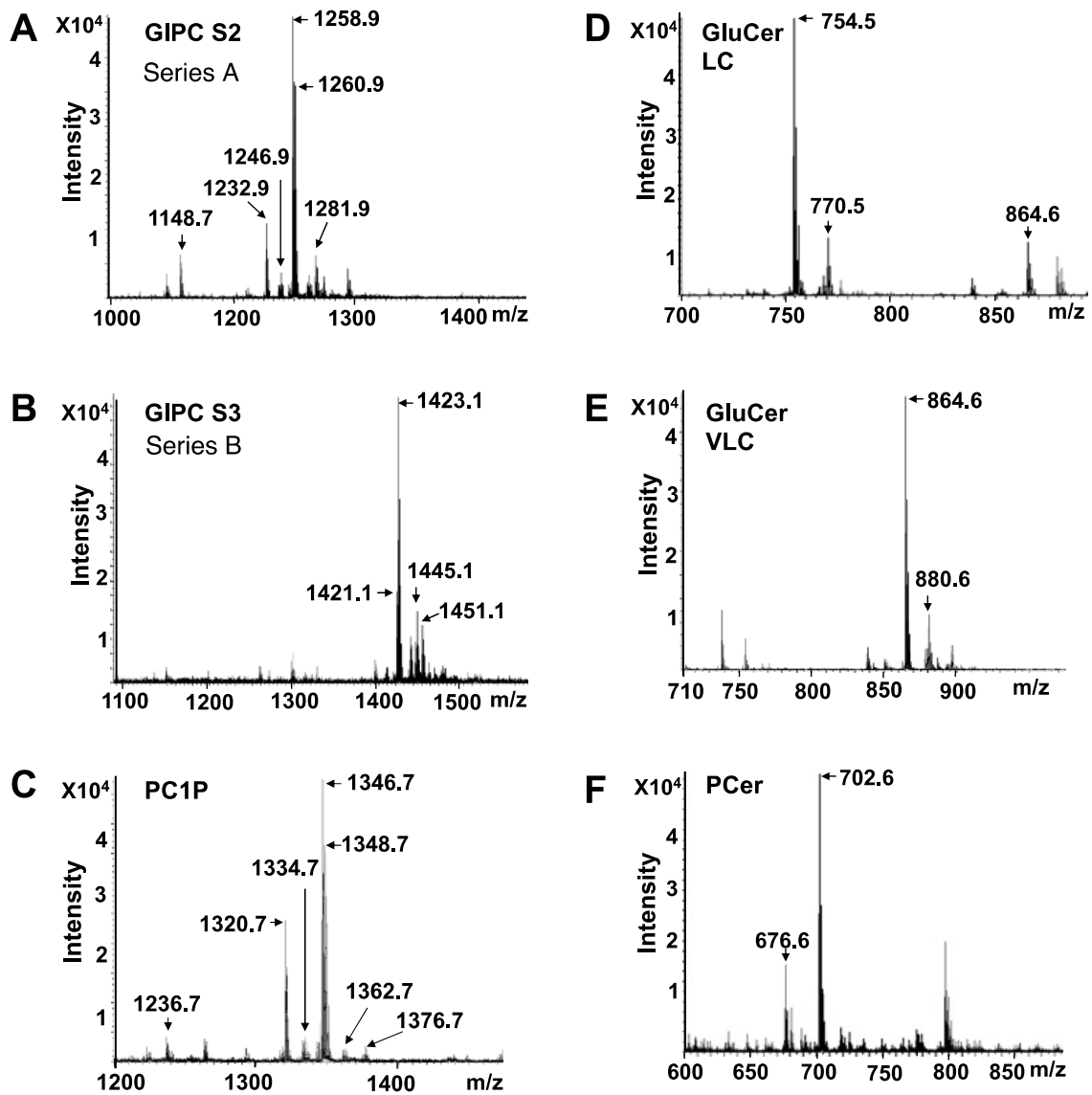


Fig. 4

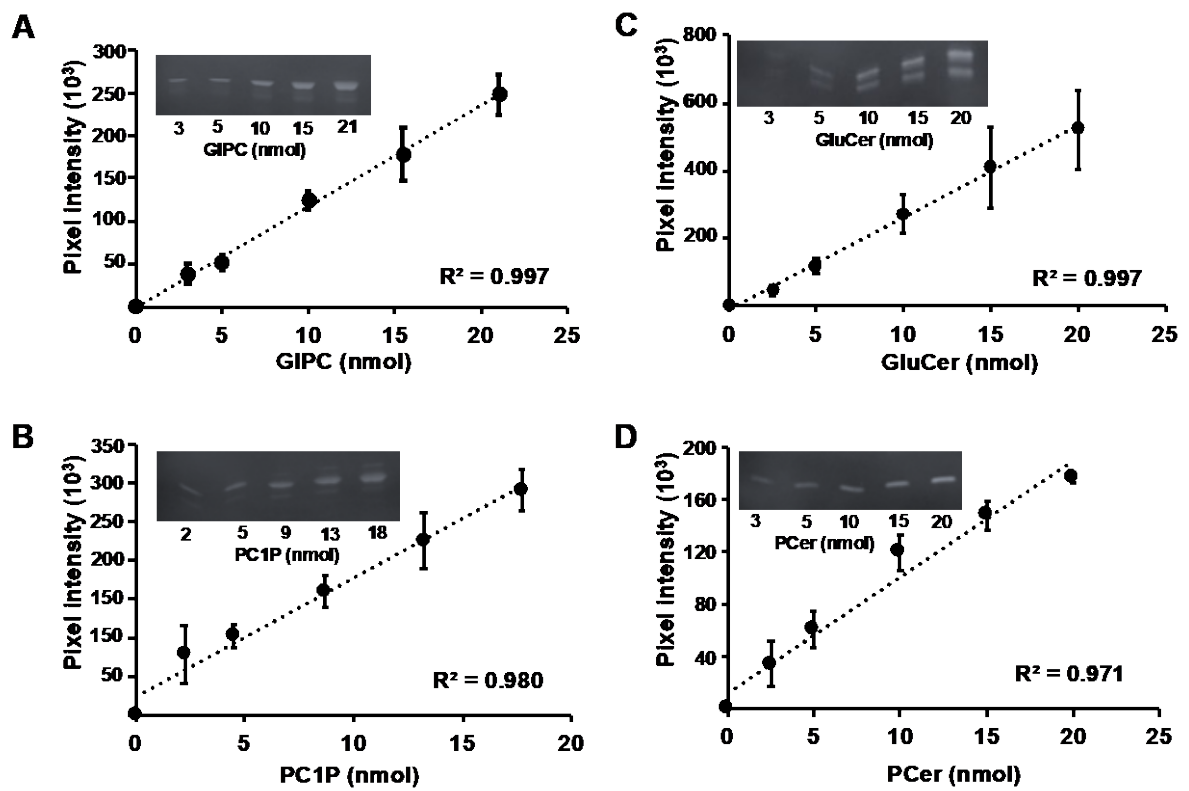


Fig. 5

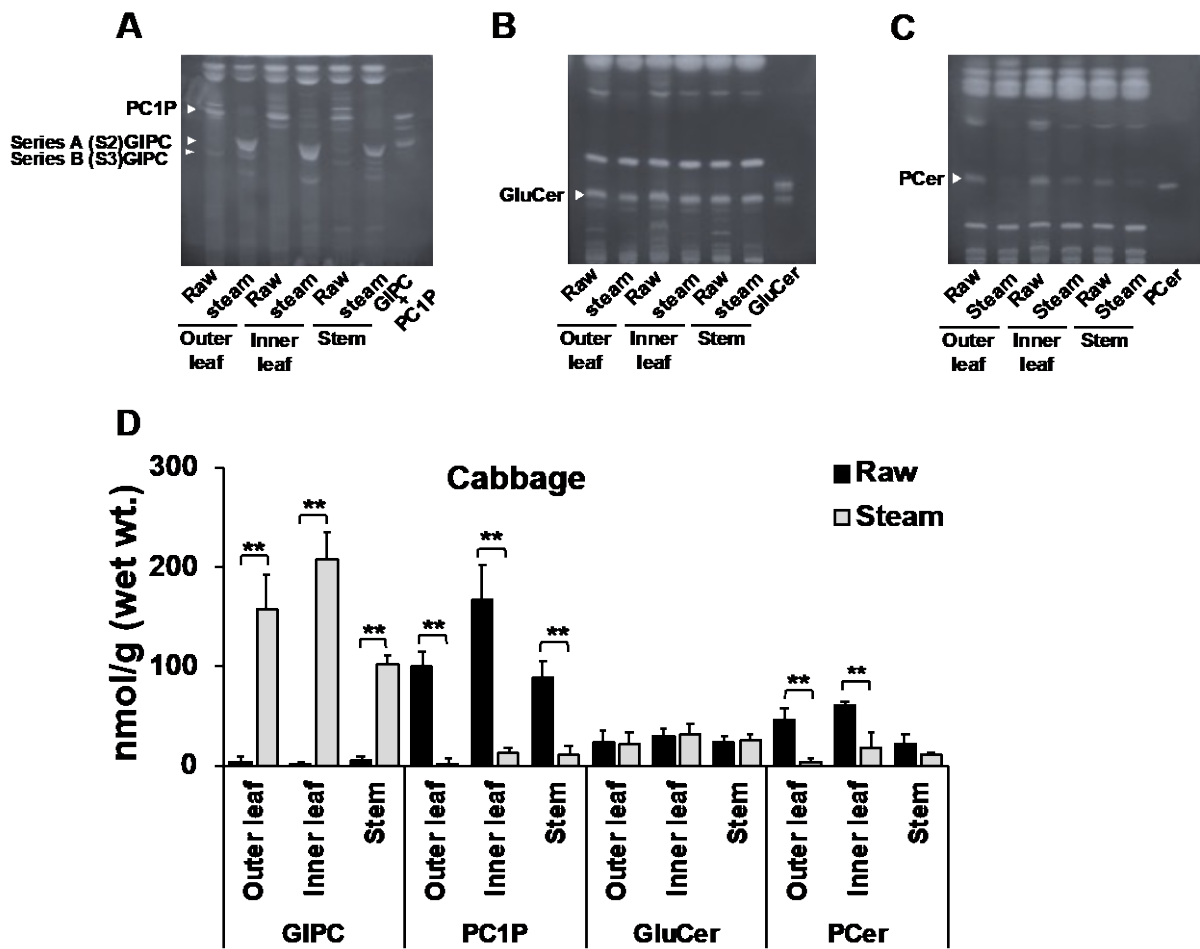


Fig. 6

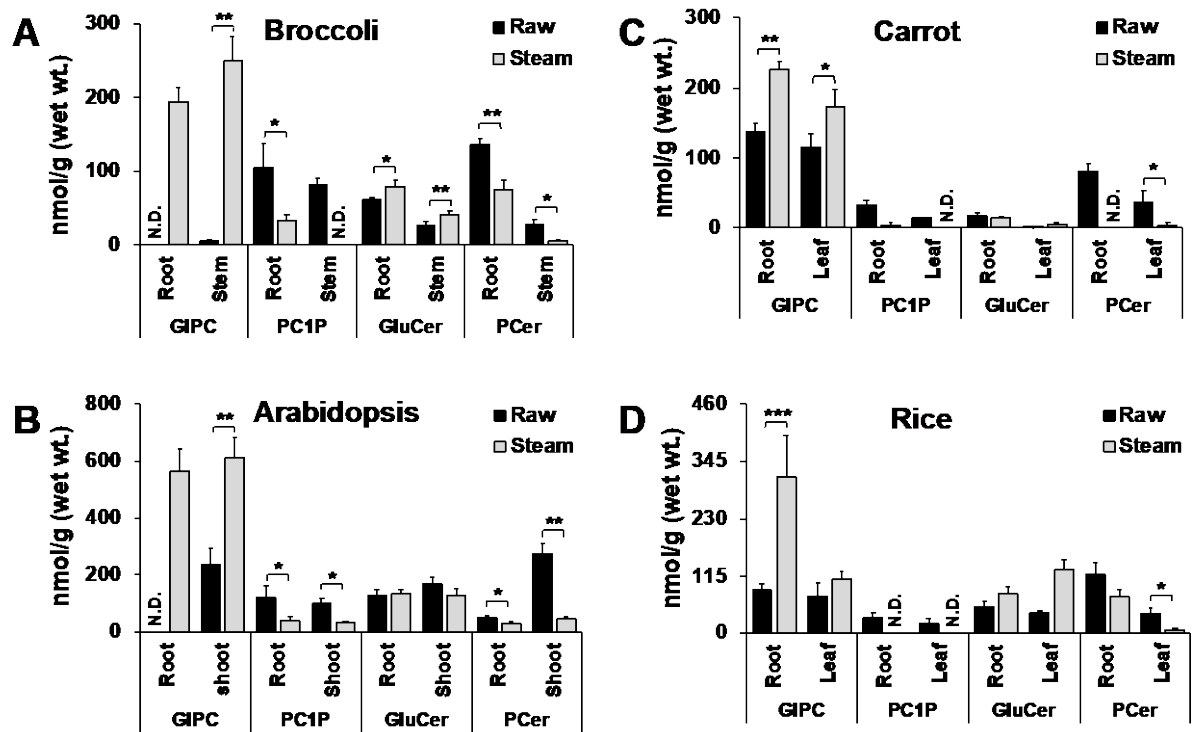


Fig.7

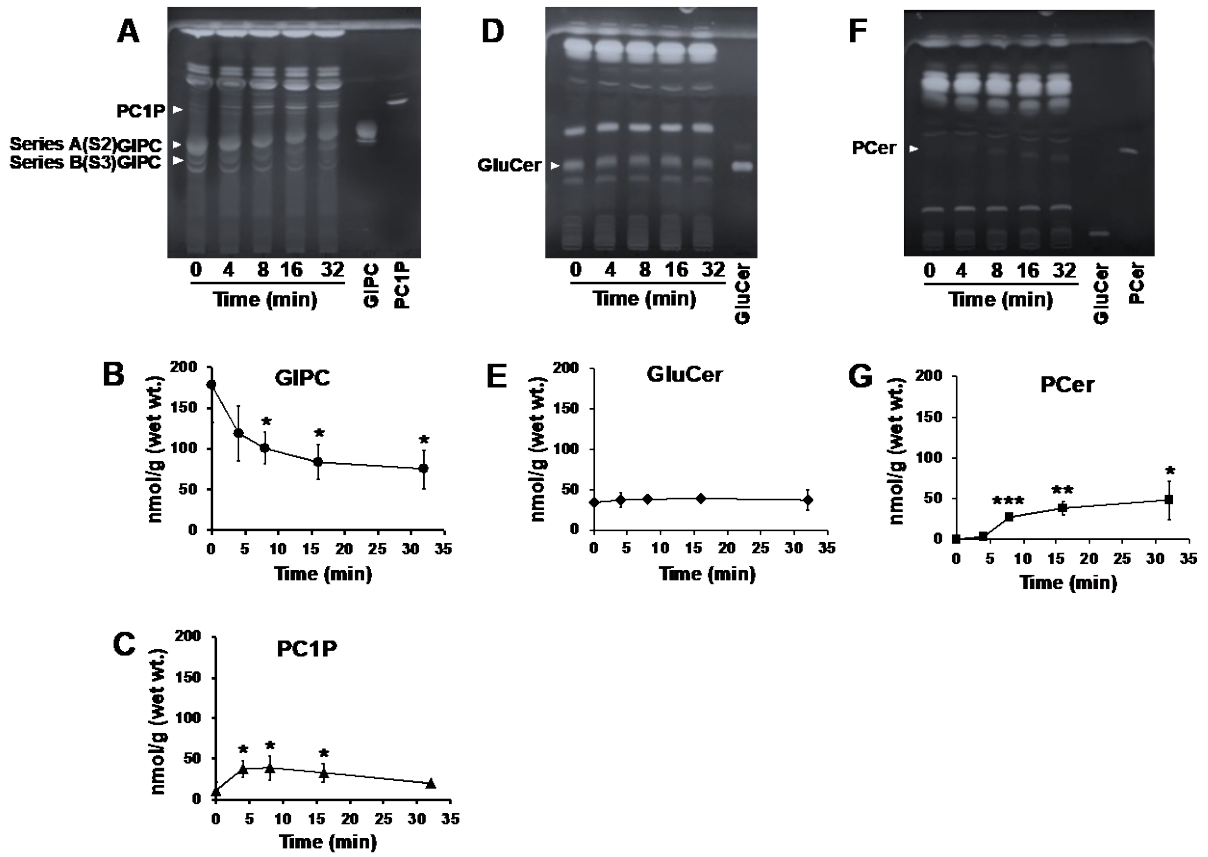
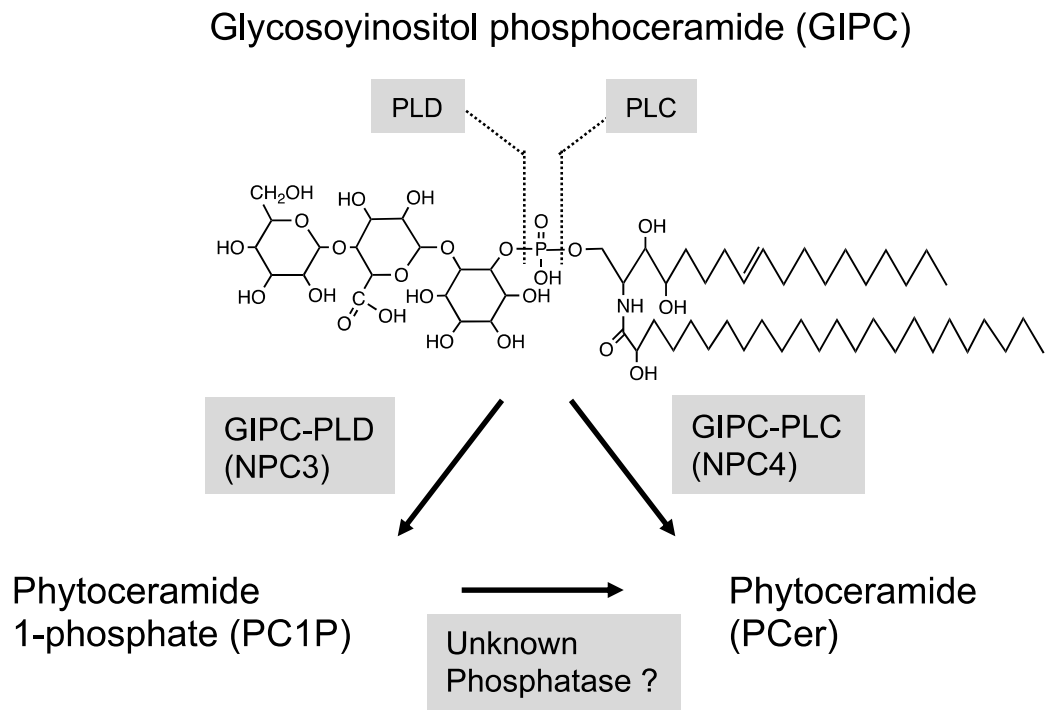
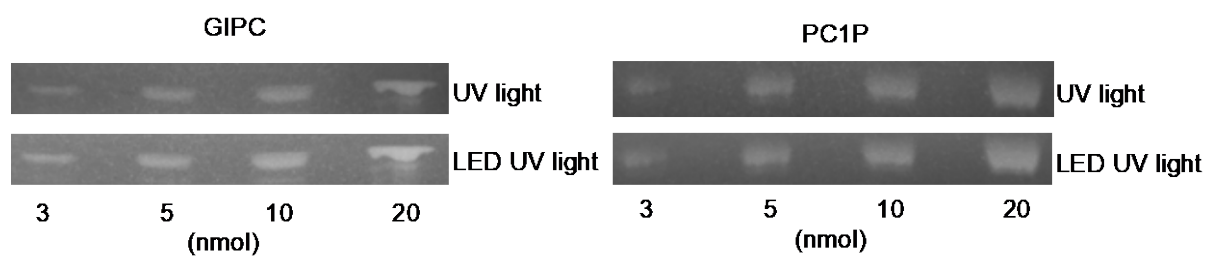


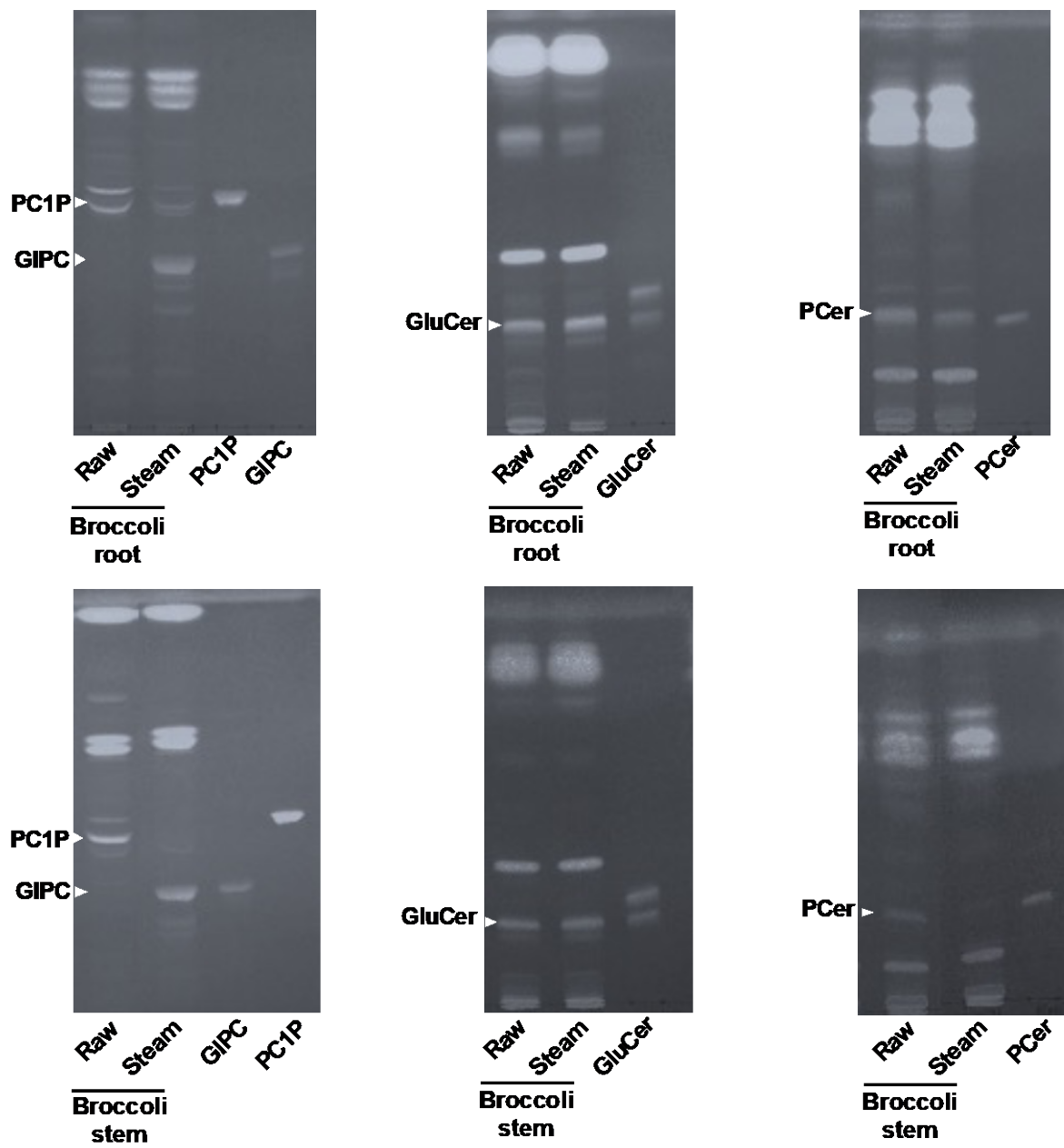
Fig. 8



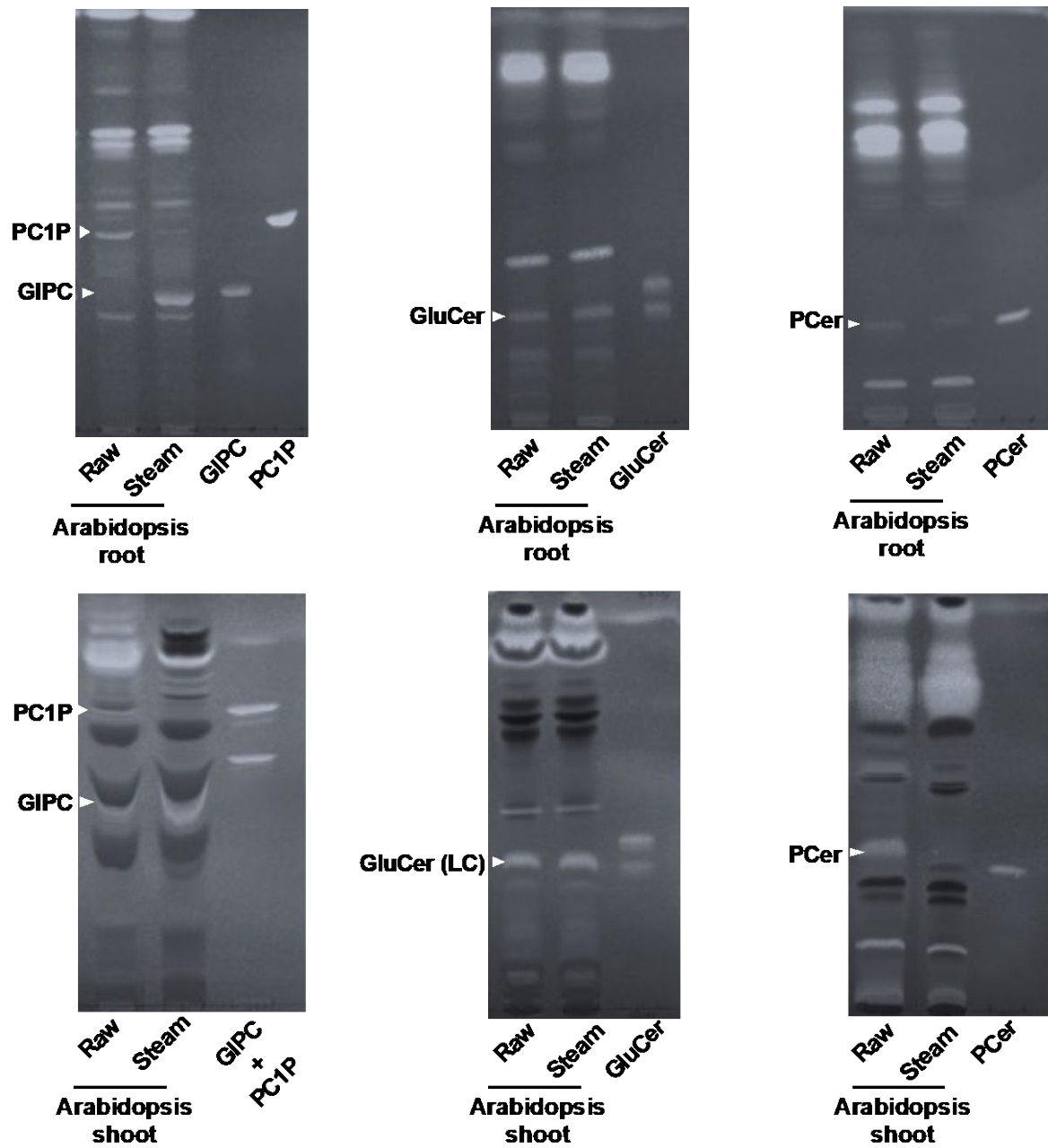


Supplementary Fig 1.

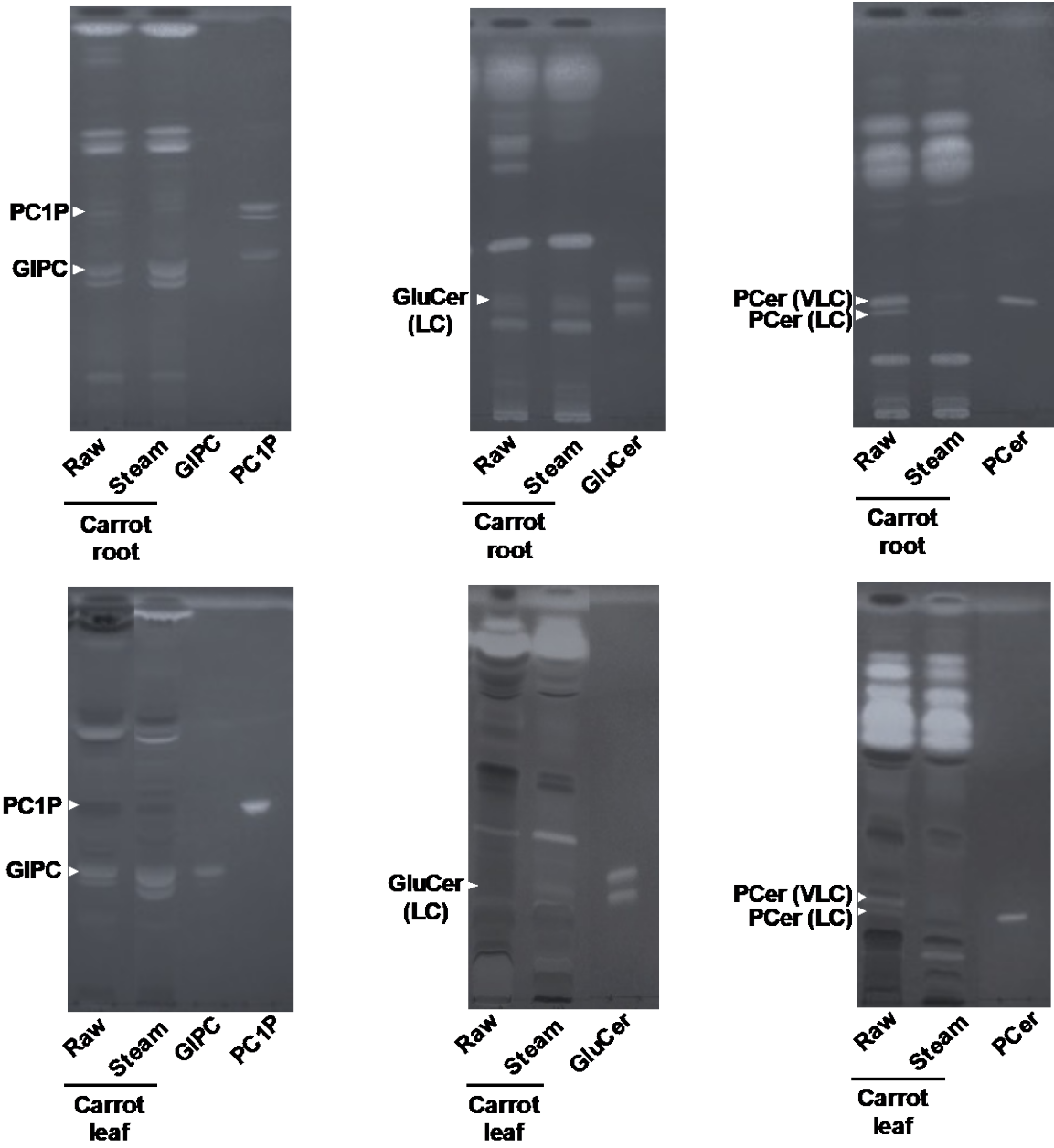
Visualization of GIPC and PC1P band on TLC with primulin/normal UV light (upper) and primulin/UV LED light (lower).



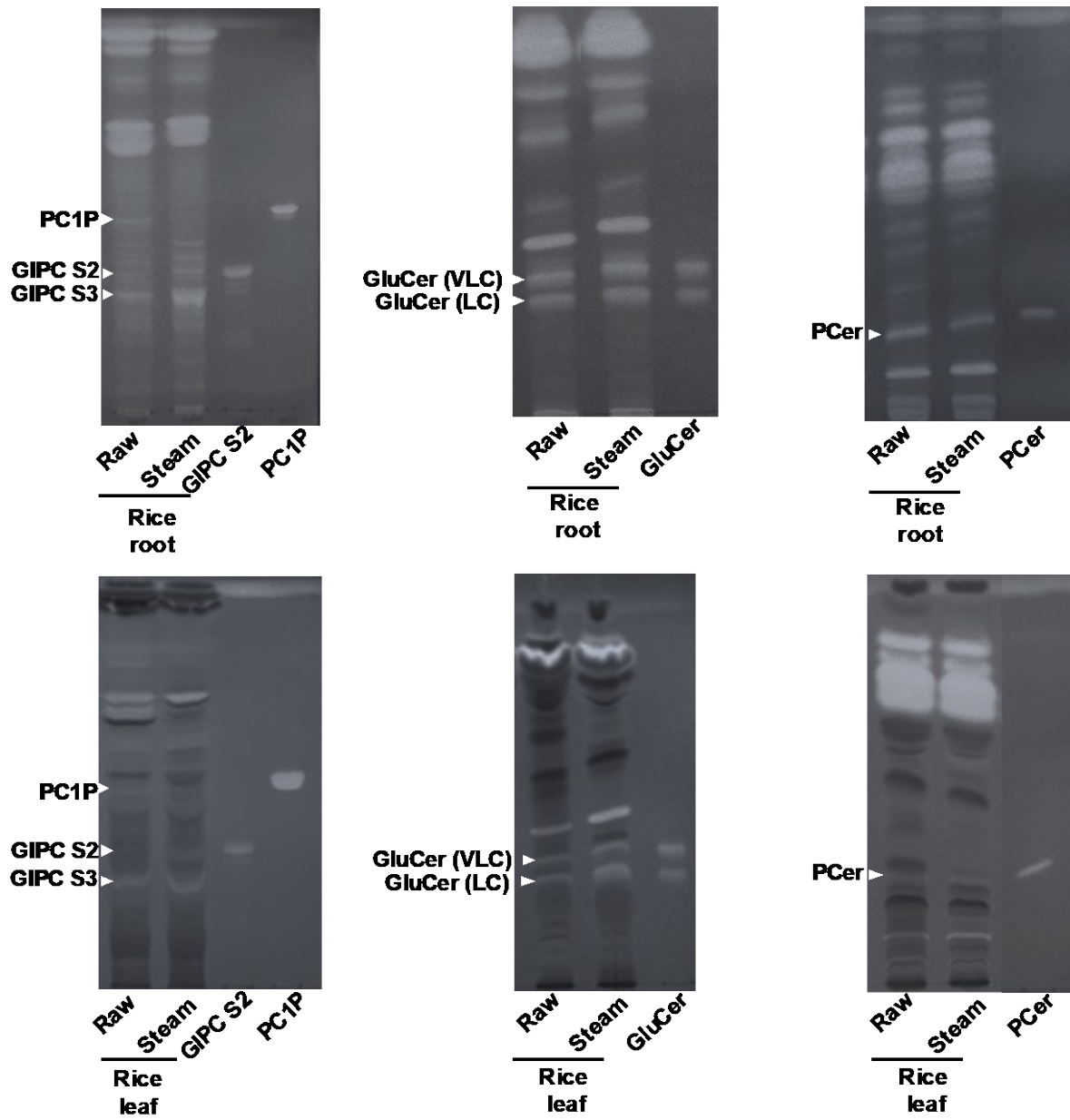
Supplement Fig. 2. Broccoli



Supplement Fig. 3. *Arabidopsis thaliana*



Supplement Fig. 4. Carrot



Supplement Fig. 5. Rice

Funding and COI

This work was supported by grants-in-aid from the Ministry of Education, Science, Sports, and Culture of Japan (19K05863 to T.T.), and the Kobayashi Foundation (to T. T.).

The authors declare no conflict of interest associated with this manuscript.